

Properties of Electrodeposited Tungsten Coatings on Graphite Substrates for Plasma Facing Components

Ningbo Sun¹ · Shaoting Lang¹ · Yingchun Zhang¹ · Yuping Xu² · Hui Liu¹ · Guangbin Li¹

Published online: 12 March 2016
© Springer Science+Business Media New York 2016

Abstract Tungsten coating on graphite substrate is considered as one of promising candidate materials of plasma facing components. In this study, tungsten coatings on graphite substrate were successfully prepared by direct current (DC) and pulse current (PC) electrodeposition methods in Na₂WO₄–WO₃ molten salt under the air atmosphere. Pores were found on the surfaces of the tungsten coatings produced by DC electrodeposition method. For the coatings fabricated by PC method, compact and smooth tungsten coatings were successfully obtained. The crystal structure, morphology, density, microhardness, adhesive strength, oxygen content and the thermal conductivity of the coatings fabricated by PC method were investigated. The obtained tungsten coatings had a body centered cubic structure. After electro-deposition for 100 h, the thickness of the tungsten coating reached $810.02 \pm 10.40 \mu\text{m}$ and the oxygen content was 0.03 wt%. The thermal conductivity of the tungsten coating was $134.29 \text{ W m}^{-1} \text{ K}^{-1}$. The density of the tungsten coating was 18.83 g cm^{-3} . The hardness of the coating was $492.0 \pm 7.8 \text{ HV}$. After deuterium plasma irradiation, the tungsten coatings were prone to blistering.

Keywords Tungsten coating · Graphite substrate · Electrodeposition · Duration · Deuterium plasma irradiation

Introduction

Due to the advantages of high melting point (the highest among the metals), good thermal conductivity and high physical sputtering threshold energy, et al. tungsten has been considered as the main candidate materials for PFCs [1, 2]. However, the critical issues of tungsten block, such as heavy weight, poor machining processing and high ductile–brittle transition temperature (DBTT), restrict its further applications. In order to mitigate these issues, an innovative approach was proposed to deposit tungsten coatings on low-Z materials (such as graphite and C/C fiber composite) [3, 4]. Nowadays, many coating techniques have been used to produce tungsten coatings on graphite substrates, i.e., physical vapor deposition (PVD), chemical vapor deposition (CVD), plasma spray (PS), combined magnetron sputtering and ion implantation (CMSII) and electrodeposition [5–7]. Among these kinds of coating technologies, electrodeposition method has unique advantages to fabricate tungsten coatings due to its simplicity, low cost and the satisfied properties of the obtained tungsten coatings [8–10].

Pure tungsten which was electrodeposited from molten salt can be traced to 1960's [11]. Nowadays, researchers are widely interested in the oxide molten salt system [12–14]. Due to its non-volatility, easily preparation, chemically stability, and broad application prospect, the Na₂WO₄–WO₃ molten salt system was considered as the most promising molten salt system to prepare pure tungsten coatings [15]. In addition, DC and PC were widely used to

Ningbo Sun and Shaoting Lang have contributed equally to this study and share the first authorship.

✉ Yingchun Zhang
zycustb111@163.com

¹ School of Materials Science and Engineering, University of Science and Technology Beijing, 30 Xueyuan Road, Haidian District, Beijing 100083, People's Republic of China

² The Institute of Plasma Physics, Chinese Academy of Sciences, P.O. Box 1126, Hefei 230031, People's Republic of China

produce metal coatings because of their simplicity [16, 17]. In this work, DC and PC were used to prepare tungsten coatings on graphite substrates from Na₂WO₄ to WO₃ molten salt system at 1173 K. Various durations were used to produce tungsten coatings. The microstructures of the electrodeposited tungsten coatings were observed. The properties of tungsten coatings prepared by PC were investigated. And the D plasma irradiation was applied on the selected tungsten coatings to investigate their irradiation properties.

Experimental

The compositions of the salts for the electrodepositing tungsten coatings were thoroughly mixed anhydrous reagent grade chemicals (Na₂WO₄:WO₃ = 3:1, by mole ratio). The electrodeposition was carried out at 1173 K using a pulse power supply (HPMCC-5). DC and PC electrodeposition methods were used to produce tungsten coatings in this work. The operating parameters for these electrodeposition methods are shown in Table 1. A graphite substrate with the dimensions of 15 mm × 15 mm × 5 mm was used as the working cathode. The anode electrode was a tungsten plate with the same dimensions as the working cathode. After the electrodeposition, the sample was cooled in air and then ultrasonic-cleaned in a 10 M NaOH solution and deionized water to remove the adherent salts.

The crystal structures of the obtained tungsten coatings were detected by X-ray diffractometer (XRD, Rigaku Industrial Co., Ltd., D/MAX-RB). The morphologies of the surfaces and cross-sections of the obtained coatings were observed by a scanning electron microscope (SEM, JSM 6480LV). The micro-hardnesses of the coatings were measured by a micro-hardness instrument (MH-6) with a loading force of 50 g and loading time of 15 s. The adhesion was detected by the coating-pull-off test according to ISO 4624:2002 (E). The oxygen content was measured by the Nitrogen/Oxygen Analyzer (TC600, LECO, USA). A flash diffusivity instrument (LFA447) was used to test the thermal conductivity of tungsten coatings. Archimedes method was applied to measure the density of tungsten coating. In order to investigate the effects of

deuterium (D) plasma irradiation on the morphologies of electrodeposited tungsten coating (with the thickness of 800 μm), the experiment was performed in the experimental advanced superconducting tokamak (EAST) at the Institute of Plasma Physics, Chinese Academy of Sciences. Before the experiment, the sample was cut into piece of 10 × 10 × 3 mm and polished and rinsed in acetone. Then the sample was fixed on the specimen platform of the material and plasma evaluation system (MAPES) at the mid-plane of EAST [18]. The sample was irradiated for 367 shots with the total plasma exposure time of 2005.3 s. The surface temperature of the sample was ranging from ~325 to 475 K due to the heating effect of the D plasmas. The local electron temperature and density were measured to be 5–20 eV and ~10¹⁸ m⁻³. The morphologies of the sample before and after D plasma irradiation were investigated by SEM.

Results and Discussion

The Crystal Structures and Morphology

Figure 1 depicts the XRD patterns of the obtained tungsten coatings produced by DC and PC in the Na₂WO₄–WO₃ melt at 1173 K for 1 h. It can be found that the crystal planes of (1 1 0), (2 0 0), (2 1 1) and (2 2 0) were corresponded to the four diffraction peaks at 2θ angles of 40, 58, 73 and 87°, respectively. This reveals that the tungsten coatings had a body-centered cubic (BCC) structure. Moreover, in Fig. 1a, three diffraction peaks of graphite were detected due to the pores on the surface of the tungsten coating obtained by DC (see in Fig. 2a). The XRD

Table 1 Electrodeposition parameters for producing tungsten coatings

	DC	PC
$r = T_{on}/(T_{on} + T_{off})$	1	0.3
I (mA cm ⁻²)	$I = 40$	$I_p = 40$
t (h)	1	1, 12, 24, 70, 100

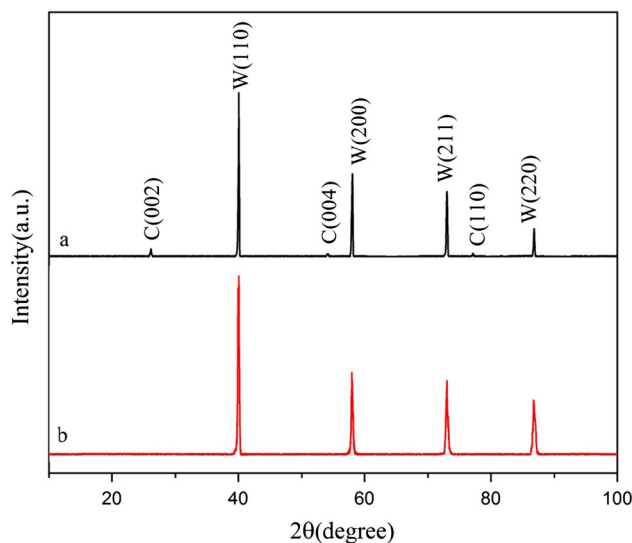


Fig. 1 XRD patterns of the tungsten coatings **a** DC, **b** PC

results demonstrated that pure and polycrystalline tungsten coatings were obtained by both methods. The main reason was due to the electrochemical processes were the same for the two methods, and the electrodeposition processes on the cathode ($4 \text{W}_2\text{O}_7^{2-} + 6\text{e} = \text{W}^0 + 7\text{WO}_4^{2-}$) were without other impurity ions. Figure 2 shows the SEM images of the obtained tungsten coatings. Pores were discovered on the surface of the coating deposited by DC, however, no observable pores were found on the tungsten coatings produced by PC. The phenomenon of poor quality (e.g. pores and pocking) of the coating deposited by DC was caused by using continuous DC [19]. The results demonstrated that PC method was more suitable for producing high quality tungsten coatings in this case.

Various Durations of PC Electrodeposition

The thickness of coating is a critical factor for the longevity of the obtained products. Various durations (Table 1) of PC electrodeposition were conducted at the same current density of 40 mA cm^{-2} and pulse duty ratio of 0.3. The SEM images of the cross-sections of the obtained coatings are shown in Fig. 3. It was obvious that uniform and crack-free tungsten coatings were obtained under all durations. And the thicknesses of these coatings increased significantly with increasing the electrodeposition time. After electrodeposited for 12 h, the thickness of the tungsten coating was achieved $271.54 \pm 6.50 \mu\text{m}$. For the duration of 24 h, the thickness of the coating reached $436.21 \pm 7.80 \mu\text{m}$. As the duration extended to 70 h, the thickness increased to $619.30 \pm 9.10 \mu\text{m}$. And the thickness of the coating reached $810.02 \pm 10.40 \mu\text{m}$ when the duration was 100 h (see Figs. 3, 4). Compared with the thickness of tungsten coating in ref. [20], the growth rate of tungsten coating on graphite substrate was higher than that of tungsten coatings on low activation steel substrate. Except for the thickness, the hardness is another important property of coatings. As shown in Fig. 5, the hardness of

the tungsten coatings showed the same tendency as the thickness. After electrodepositing for 12, 24, 70 and 100 h, the hardness of the coatings reached 457.0 ± 5.3 , 475.0 ± 8.2 , 480.0 ± 7.4 and $492.0 \pm 7.8 \text{ HV}$, respectively. The main reason for the increase of the hardness was the reduction of the effect of graphite substrate with increasing coating thickness. As is well known, thick coatings were always preferred for the coating products. In this case, the tungsten coatings obtained after 100 h electrodeposition was the best scenario for the D irradiation test.

Properties of the Thick Tungsten Coatings

The physical properties of the tungsten coatings with the thickness of $810 \mu\text{m}$ are listed in Table 2. The average tensile adhesive strength between the coating and graphite substrate was 26 MPa. It was lower than the adhesive strength of the coatings on V-4Cr-4Ti and copper obtained by electrodeposition [12]. This was due to the less stable adhesive strength between metals and non-metals than that between metals. As is well known, low-oxygen content was beneficial for prolonging the service life of coating products, especially for the PFCs. The oxygen content of the tungsten coating with thickness of $810 \mu\text{m}$ was 0.03 wt% which was much lower than that of tungsten coatings prepared by plasma spraying (PS) method [21, 22]. It was due to that the electrochemical process in the molten salts was an anaerobic condition. No exotic oxygen ions from outside environment were introduced. The low oxygen content was mainly caused by the slightly oxidation of tungsten coatings after the sample was taken out from the molten salts and cooled in the air.

The density of the thick tungsten coating was determined to be about 18.83 g cm^{-3} . The thermal diffusivity was tested in the room temperature using a tungsten coating wafer with a diameter of 25.40 mm. The thermal diffusivity was tested to be about $54.86 \text{ mm}^2 \text{ s}^{-1}$ which was higher than that of the vacuum plasma sprayed (VPS)

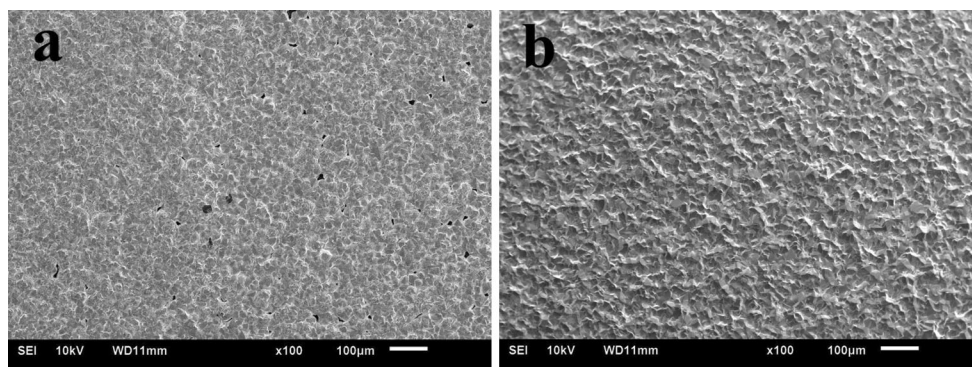


Fig. 2 The SEM images of electrodeposited tungsten coatings **a** DC, **b** PC

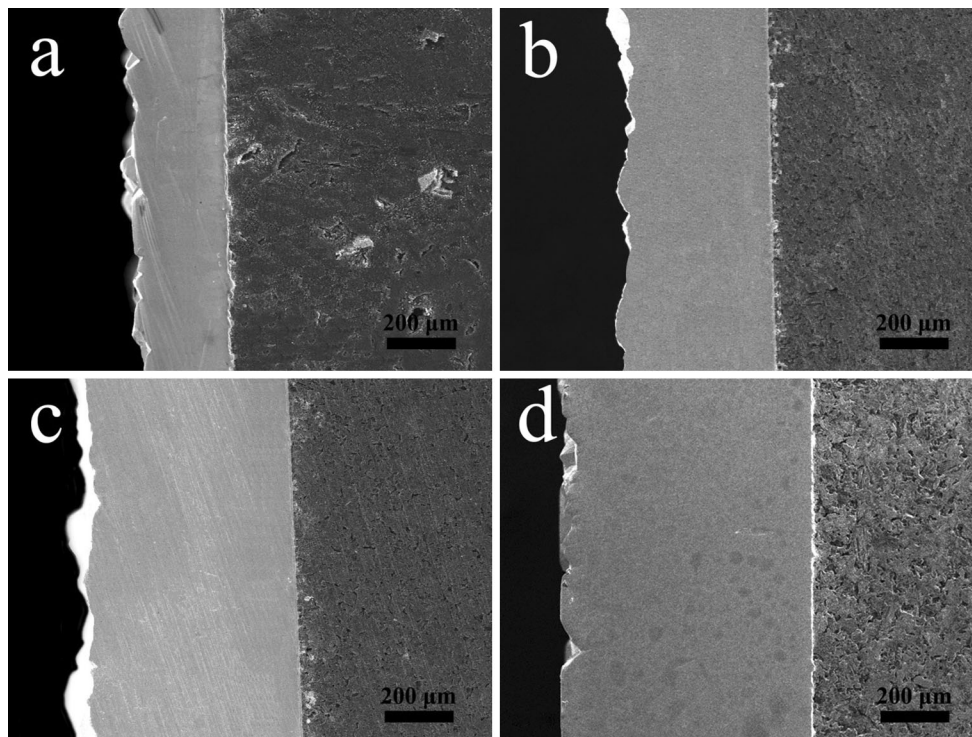


Fig. 3 The cross-section SEM images of tungsten coatings obtained at **a** 12 h, **b** 24 h, **c** 70 h, **d** 100 h

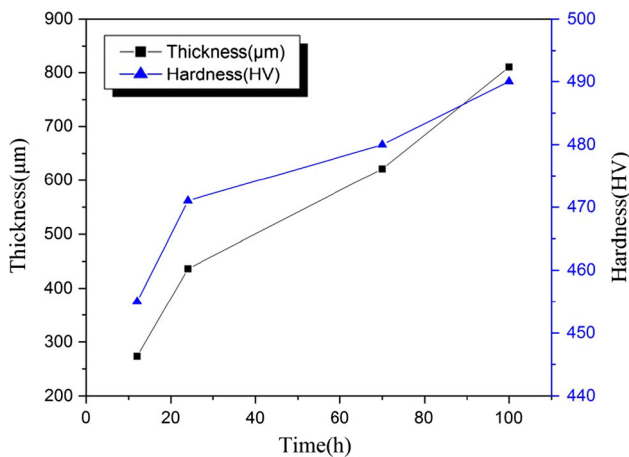


Fig. 4 The thickness and hardness of tungsten coatings obtained at 12, 24, 70, 100 h

tungsten coating about $47.70 \text{ mm}^2 \text{ s}^{-1}$ [19]. The thermal conductivity was calculated by the following equation:

$$k = \rho \times C_p \times \alpha \tag{1}$$

Where k is the thermal conductivity, ρ is the density of the coating (18.83 g cm^{-3}), C_p is the coatings' specific heat ($0.13 \text{ J g}^{-1} \text{ K}^{-1}$) and α is the thermal diffusivity of the coating. So this implied that the density of the coating had significant influence on the thermal conductivity. The thermal conductivity of the obtained thick tungsten coating

reached $134.29 \text{ W m}^{-1} \text{ K}^{-1}$, which was much higher than that of the tungsten coatings prepared by N. Yaran ($108 \text{ W m}^{-1} \text{ K}^{-1}$) using VPS method [23]. This was mainly caused by the high density and the high quality (no cracks and pores in the microstructure) of the obtained coatings.

D Plasma Irradiation

The thick tungsten coating (810 μm) has been irradiated for 367 shots with the total plasma exposure time of 2005.3 s using D plasma. The surface SEM images of the sample before and after exposure to D plasma were shown in Fig. 5. As can be seen, mechanical polished surface of the samples before exposure to D plasma was smooth, crack-free and astomatous. After the irradiation, pores with few tens nanometer were distributed uniformly on the whole surface of the tungsten coating. Moreover, blisters with the size ranging from hundreds to thousands of nanometers were detected on the coating surface. No microcracks were found on the surface of blisters with submicron sizes. However, when the size of the blisters reached micron-scale, microcracks appeared on the surface of the blisters. And the amount and the width of the microcracks increased with increasing of the size of the blisters. Tungsten has a very low solubility for hydrogen. When the concentration of interstitial D exceeded the

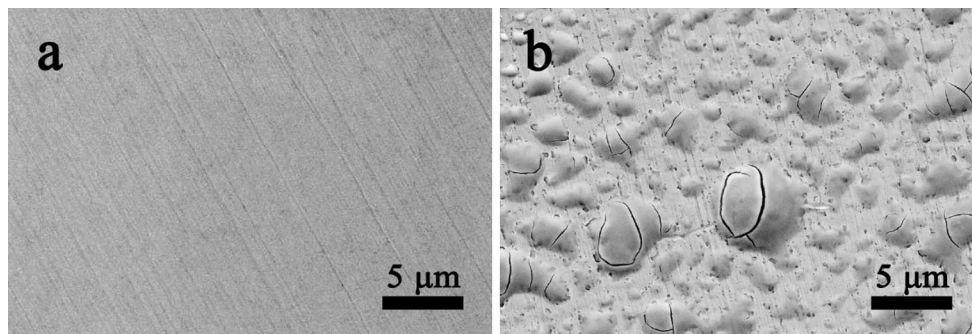


Fig. 5 The surface SEM images of the sample **a** before and **b** after been exposed to D plasma

Table 2 Properties of the tungsten coating with the thickness of 810 μm

Properties	Values
Adhesive strength (MPa)	26 ± 4.32
Oxygen content (wt%)	0.03
Thermal conductivity (W m ⁻¹ K ⁻¹)	134.294
Density (g cm ⁻³)	18.83

solubility during the irradiation, D started to precipitate and accumulated at the dislocations, grain boundaries and vacancies of the irradiated layers. And as a result, a large number of nano-blisters would form [24]. As the irradiation time increased, the nano-blisters would merge and grow up simultaneously, which resulted in the increasing of the pressure inside the blister. Obvious blisters with large sizes would appear at the W coating surface when the inner pressure exceeded the yield strength of tungsten. With the inner pressure continued to increase and exceeded the breaking strength of tungsten, cracking of the blisters would appear on the surface [25–27]. In short, the tungsten coatings were prone to blistering under D irradiation [28].

Conclusion

Pure tungsten coatings were successfully produced on graphite substrates by DC and PC electrodeposition methods from Na₂WO₄ to WO₃ molten salts in the air at 1173 K. Pores were detected on the surface of tungsten coating obtained by DC. Pure, uniform and crack-free tungsten coatings were successfully obtained by PC. The thicknesses of these coatings increased with increasing the electrodeposition time. The maximum thickness of the tungsten coatings on graphite substrates was measured to be 810.02 ± 10.40 μm with the electrodeposition duration of 100 h. The hardness of the coatings reached 492 ± 7.80

HV after electrodeposition for 100 h. And the bonding between tungsten coating and graphite substrate was compact. The average tensile adhesive strength between the coating and graphite substrate was 26 MPa. The 0.03 wt% oxygen content was at a very low level. The density and thermal conductivity of the tungsten coating were 18.83 g cm⁻³ and 134.29 W m⁻¹ K⁻¹, respectively. After D irradiation, nano sized pores were distributed uniformly on the whole surface of the tungsten coatings and the coatings were prone to blistering. Microcracks appeared on the surface of the blisters with the size in micron-scale.

Acknowledgments The study was supported by ITER-National Magnetic Confinement Fusion Program (No. 2014GB123000) and the National Natural Science Foundation of China. (Nos. 51172019, 51372017).

References

1. H. Kim, J. El-Awady, V. Gupta et al., *J. Nucl. Mater.* **386**, 863–865 (2009)
2. C. Ruset, E. Grigore, H. Maier et al., *Fusion Eng. Des.* **86**, 1677–1680 (2011)
3. P.T. Lang, A. Kallenbach, J. Bucalossi et al. in *Integrated exhaust scenarios with actively controlled ELMs, 20th IAEA Fusion Energy Conference*, Vilamoura, Portugal, 2004
4. C. Ruset, E. Grigore, I. Munteanu et al., *Fusion Eng. Des.* **84**, 1662–1665 (2009)
5. M.T. Hosseinejad, M. Shirazi, Z. Ghorannevis et al., *J. Fusion Energy.* **31**(5), 426–431 (2012)
6. C. Ruset, E. Grigore, H. Maier, R. Neu, X. Li, H. Dong et al., *Phys. Scr.* **T128**, 171–174 (2007)
7. N. Sun, Y. Zhang, F. Jiang, S. Lang, *Fusion Eng. Des.* **89**, 2529–2533 (2014)
8. I. Kosta, E. Vallés, E. Gómez, M. Sarret, C. Müller, *Mater. Lett.* **65**, 2849–2851 (2011)
9. H. Alimadadi, M. Ahmadi, M. Aliofkhaezraei, S. Younesi, *Mater. Des.* **30**, 1356–1361 (2009)
10. F. Jiang, *Appl. Surf. Sci.* **363**, 389–394 (2016)
11. S. Senderoff, G.W. Mellors, *Science* **153**, 1475–1481 (1966)
12. Y. Liu, Y. Zhang, Q. Liu, *Fusion Eng. Des.* **87**(11), 1861–1865 (2012)
13. Y. Liu, Y. Zhang, Q. Liu, *Rare Met.* **31**(4), 350–354 (2012)

14. F. Jiang, Y.C. Zhang, N. Sun, Appl. Surf. Sci. **331**, 278–284 (2015)
15. V.V. Malyshev, Prot. Met. **37**, 216–222 (2001)
16. B.G. An, L.X. Li, H.X. Li, Mater. Chem. Phys. **110**, 481–485 (2008)
17. Y. Suzuki, S. Arai, M. Endob, Appl. Surf. Sci. **256**, 6914–6917 (2010)
18. D. Fang, G. Luo et al., J. Nucl. Mater. **455**, 710–716 (2014)
19. R.A. Zhu, *Pulse Electrodeposition* (Publishing House of Electronics Industry of China, Beijing, 1986), p. 7
20. N. Sun, Y.C. Zhang, S. Lang, J. Fusion Energ. **34**, 1417–1422 (2015)
21. J.J. Huang, X.J. Li, J. Chen, Y. Liu et al., J. Nucl. Mater. **432**, 16–19 (2013)
22. F.L. Chong, J.L. Chen, J.G. Li et al., J. Nucl. Mater. **375**, 213–217 (2008)
23. Y. Niu, X. Zheng, H. Ji et al., Fusion Eng. Des. **85**, 1521–1526 (2010)
24. M.H.J. 't Hoen, M. Balden, A. Manhard et al., Nucl. Fusion **54**, 083014 (2014)
25. M. Balden, A. Manhard, S. Elgeti, J. Nucl. Mater. **452**, 248–256 (2014)
26. L. Buzi, G. De Temmerman, B. Unterberg et al., J. Nucl. Mater. **463**, 320–324 (2015)
27. J.B. Condon, T. Schober, J. Nucl. Mater. **207**, 1–24 (1993)
28. L. Buzi, G.D. Temmerman, B. Unterberg, J. Nucl. Mater. **455**, 316–319 (2014)